Polymer Chemistry

PAPER

View Article Online
View Journal | View Issue



Cite this: *Polym. Chem.*, 2018, **9**, 5385

# Giant polymersomes from non-assisted film hydration of phosphate-based block copolymers†

Emeline Rideau, Frederik R. Wurm * and Katharina Landfester *

Received 3rd July 2018,
Accepted 9th October 2018

DOI: 10.1039/c8py00992a

rsc.li/polymers

The self-assembly of amphiphilic block copolymers is a fast way to prepare chemically versatile and stable "protocells" that can act as a reactor or a confinement. However, controlling their self-assembly into giant unilamellar vesicles (GUVs) with diameters of several micrometers is challenging. Electroformation has been used to generate GUVs from amphiphilic block copolymers, which can be studied by light microscopy and resemble cell-like entities. However, a mild film hydration protocol for GUV preparation would be desirable in order to prepare libraries of protocells for further applications. Here, we present the self-assembly of novel amphiphilic polybutadiene-*block*-polyphosphoester block copolymers into GUVs by simple film hydration. These amphiphiles are synthetic analogs of phospholipids and possess the hydrophilic poly(ethylene ethyl phosphate) (PEEP) block. The GUVs (with diameters of *ca.* 10–40 μm) were formed in high yields by simple non-assisted film hydration requiring no external forces and with no need of the commonly applied electroformation. PEEP-based block copolymers with a lamellar bulk morphology produced GUVs in high yields and outperformed commonly used block copolymers (*e.g.* with poly(ethylene oxide) as a hydrophilic segment). We quantified their respective yield (number of GUVs formed) and diameters and monitored their stability over time. In addition, we proved their encapsulation capacity and permeability to hydrophobic and hydrophilic fluorescent cargo. Due to their high performance, these phosphate-based amphiphilic block copolymers are promising candidates for the generation of protocells and self-assembled microreactors.



## Introduction

Compartmentalization of cells is a key feature of life.[1,2] The plasma membrane is composed of a complex, balanced ratio of lipids, proteins, and small molecules and has many functions.[3] Cell membrane mimicking has become an important quest for simplifying the understanding of the membrane's inherent properties, functions and behaviors[4–6] as well as for using their biocompatibility to expand drugs' bioavailability, medical imaging and diagnostics[7–9] or to compartmentalize incompatible entities in the synthesis.[2,10]

Cell membrane mimicking was originally achieved with liposomes, and despite their resemblance to cell membranes, these vesicles are difficult to use and specialize, as they are unstable, fluid, and permeable.[10–13] More recently, polymeric vesicles (polymersomes) have gained in popularity, as block copolymers are chemically more versatile, malleable, and tougher than lipids, resulting in easily functionalizable, more stable vesicles.[11,13,14] Classically, polymersomes are generated from commercially available block copolymers and almost always using poly(ethylene oxide) (PEO) as the hydrophilic block.[15] A shortcoming of polymersomes is their lower biocompatibility and mimicry of cell membranes compared to liposomes as they are constituted entirely of synthetic entities.[13] In this study, we propose a novel block copolymer, namely polybutadiene-*b*-poly(ethylene ethyl phosphate) (PB-*b*-PEEP). The EEP block is interesting as its phosphate moiety resembles natural phospholipids and is biodegradable, bridging the gap between liposomes and polymersomes.[16,17] Despite this advantage, polymersomes bearing phosphate moieties are rare.[18,19] PB is also commonly used as the hydrophobic block in polymersomes as it has a low glass transition temperature ($T_g$) ($T_g \approx -21$ °C for $M_n$ = 105k; $T_g \approx -77$ °C for $M_n$ = 50k).[20] Low $T_g$ materials are desirable, as they are flexible under the self-assembly conditions (room temperature or above) and thus are able to mimic the fluidity of biomembranes contrary to more rigid hydrophobic blocks like polystyrene.[13,21,22]

The vast majority of studies on polymersomes focus on small vesicles of *ca.* 100 nm diameters, the so-called small or large unilamellar vesicles (SUVs and LUVs, respectively) as they are readily achievable by multiple methodologies.[23] However, cells are much larger (~10–100 μm) and giant unilamellar vesi-

*Max-Planck-Institut für Polymerforschung, Ackermannweg 10, 55128 Mainz, Germany. E-mail: wurm@mpip-mainz.mpg.de*

†Electronic supplementary information (ESI) available. See DOI: 10.1039/c8py00992a

cles (GUVs) (>1 μm) are thus better mimics than SUVs.[24] As increasing evidence suggests that factors such as the membrane curvature, effective encapsulated volume, stability, and permeability differ depending on size, efficient formation of GUVs becomes necessary.[25,26]

Polymeric-GUVs are more challenging to obtain than SUVs and are often generated with microfluidic devices. This controlled water-in-oil-in-water double emulsion technique selectively forms vesicles of any size in very low polydispersity.[20,27–29] However, this solvent displacement method requires complex mixtures of additives, which can be difficult to adapt to new conditions and contaminate the vesicles (*e.g.* the remaining solvent, surfactants, and additives in the membrane or in the lumen), significantly changing the membrane properties.[27,30–32] Solvent- and additive-free methodologies generating GUVs are still desirable for the robust and high-yield formation and encapsulation. Film hydration methods are based on the initial formation of a thin layer of the amphiphile on a surface by solvent evaporation followed by hydration of this solvent-free film.[14,20,23] It is generally accepted that simple hydration of amphiphilic block copolymer films does not result in polymersome formation, and especially no GUVs are obtained by this procedure.[24,31,33,34] Water cannot penetrate the dry polymer film to induce the self-assembly. Forces are required to enhance the film hydration of amphiphilic block copolymers or lipids. Commonly, shear forces like sonicating or stirring lead to SUVs or LUVs and alternative current (AC) or the use of swelling hydrogel substrates to GUVs.[31,34–37]

The exact mechanism behind the effect of AC on vesicle formation is not well understood. Despite the success of the so-called electroformation, that is, the AC-aided film hydration, for liposomes, this technique has been used only in a few studies for assembling polymeric-GUVs.[35,38–41] In the case of hydrogel-mediated hydration, the amphiphilic film is formed on a pre-dehydrated hydrophilic polymer or gel (such as poly(vinyl alcohol) or agarose). Hydration of the gel causes deformation of the amphiphilic film as a driving force for the formation of vesicles. Hydrogel-mediated polymersome formation has only been rarely described[42] and can also cause undesired membrane alteration.[31] Therefore, since the initial report of polymeric GUVs in 1999,[35] there is a clear niche for methods to form solvent and additive-free polymeric GUVs.

In this study, we first generated a library of amphiphilic PB-*b*-PEEP by sequential anionic polymerization. Then, we describe how with the appropriate block ratio PB-*b*-PEEP can generate GUVs by electroformation and even by spontaneous non-assisted direct hydration of their film within only 1 h. We quantified their yield and mean diameter, examine their stability in terms of number and size evolution over a month, and finally their encapsulation capacity to hydrophobic and hydrophilic fluorescent dyes. All these factors proved the polyphosphate-based block copolymers to be efficient amphiphiles for polymersome formation and encapsulation, superior to the commonly used block copolymers.

# Results and discussion

## PB-*b*-PEEP synthesis

PB-*b*-PEEP block copolymers were synthesized by sequential anionic polymerization (Scheme 1). The first step was the anionic polymerization of 1,3-butadiene, initialized by organolithium reagents and end-capped with ethylene oxide (EO) to yield a hydroxyl-functionalized PB-macroinitiator (PB-OH) (a).[43,44] Preferential 1,2- or 1,4-polymerization can be achieved by using THF or cyclohexane, respectively. With cyclohexane, we obtained PB-OH with 92% 1,4-microstructure (PB(1,4)-OH) (Fig. 1ii) with a low molar mass dispersity ($Đ$ = 1.06) (Fig. 1i). The degree of polymerization of PB-OH was determined by

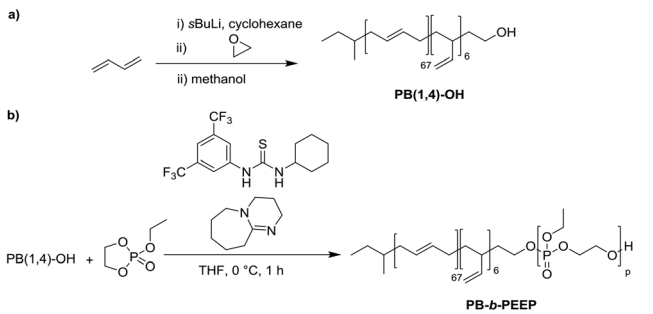


**Scheme 1** Synthesis of polybutadiene-*b*-poly(ethylene ethyl phosphate) (PB-*b*-PEEP). (a) Initial living anionic polymerization of butadiene to generate hydroxyl terminated 1,4-rich polybutadiene (PB(1,4)-OH). (b) Organocatalyzed anionic ring-opening polymerization of ethylene ethyl phosphate to the amphiphilic block copolymers PB-*b*-PEEP.

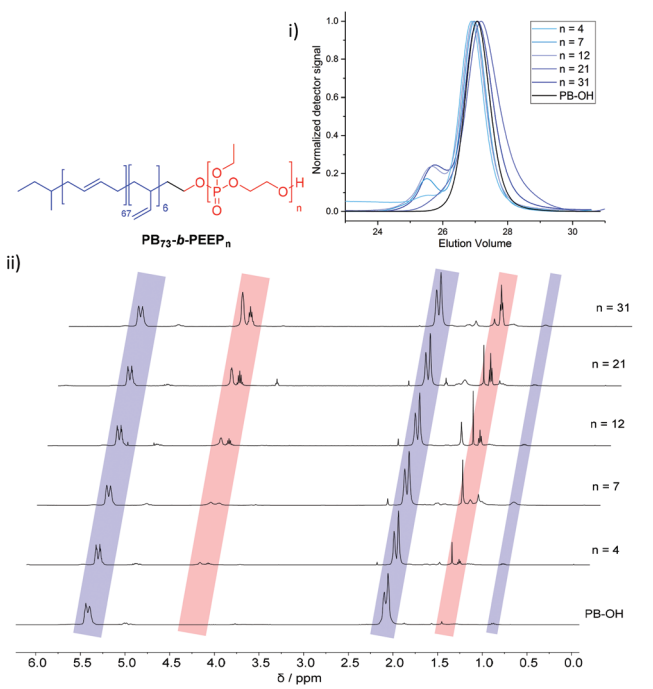


**Fig. 1** Stacked GPC curves: (i) $^1$H NMR spectra and (ii) of PB-OH and $PB_{73}$-*b*-$PEEP_n$ with the corresponding signal assignments.

NMR with reference to the methyl end-groups at 0.87 ppm (Fig. 1ii).

PB(1,4)-OH was then used to polymerize ethyl ethylene phosphate (EEP) in the presence of 1,8-diazabicyclo[5.4.0] undec-7-ene (DBU) as a base to activate the macroinitiator and a thiourea cocatalyst (b).[16] These additives reduce side reactions such as the transesterification of the EEP moiety.[16] Transesterification could still be observed as a small shoulder in the GPC curves at lower elution volume than the desired block copolymer (Fig. 1i). The shoulder appeared more prominent when targeting a higher degree of polymerization. Despite the transesterification side-reaction, all block copolymers were obtained with a narrow molar mass dispersity $Đ$ ($Đ < 1.2$) (Fig. 1i).

In comparison, classically used amphiphilic block copolymers consisting of a hydrophilic PEO block are synthesized by anionic ring-opening polymerization of the gas ethylene oxide (EO) at elevated temperature, high pressure, overnight onto the hydrophobic macroinitiator, such as PB-OH for PB-*b*-PEO.[43] However, EO is a carcinogenic, colorless, flammable gas and special care has to be taken when handled in the lab.[45] Therefore, the synthesis of PB-*b*-PEEPs is simpler, faster, and less toxic than that of PB-*b*-PEOs.

We generated a library of PB-*b*-PEEPs with a range of hydrophilic fractions $f$ ($f$ = $M_n$(hydrophilic block)/$M_n$(block copolymer)) (Fig. 1ii B–F and Table 1). The degree of hydrophilicity $f$ of amphiphilic block copolymers is an important property as it determines which macromolecular self-assembly is entropically favored.[10,15,46,47] The nature of the polymer blocks and $f$ determines their self-assembly morphologies (micelles, cylindrical micelles (worms), reverse micelles, lamellae, vesicles, *etc.*). As a general rule $0.25 < f < 0.45$ yields polymersomes[11,48] and our library is well within these boundaries. The $f$ values of each block copolymer were determined by comparing their PB(1,4) signal at 5.39 ppm (Fig. 1ii) already established for the PB-OH macroinitiator with the $CH_2$–O signals at 4.34–4.10 ppm (Fig. 1ii) of the PEEP block. These values were then used to determine the respective $M_n$ of each block copolymer.

### PB-*b*-PEEP self-assembly into GUVs by electroformation

Using our homemade electro-chamber with Pt wires (Fig. 2) we tested our library of PB-*b*-PEEPs for GUV formation by electroformation (EF) following a modified method of Discher (see ESI† pS22 for details).[35] $PB_{73}$-*b*-$PEEP_{12}$ **A** (entry 3) and $PB_{73}$-*b*-$PEEP_{21}$ **B** (entry 4) gave GUVs in high yields. Other ratios outside these boundaries yielded no vesicles. Therefore, PB-*b*-PEEPs behave similarly to other classical amphiphilic block copolymers, although they appear to favor slightly above average $f$ for vesicles as $PB_{73}$-*b*-$PEEP_7$ ($f$ = 0.21) did not self-assemble into GUVs while $PB_{73}$-*b*-$PEEP_{21}$ **B** ($f$ = 0.45) did.

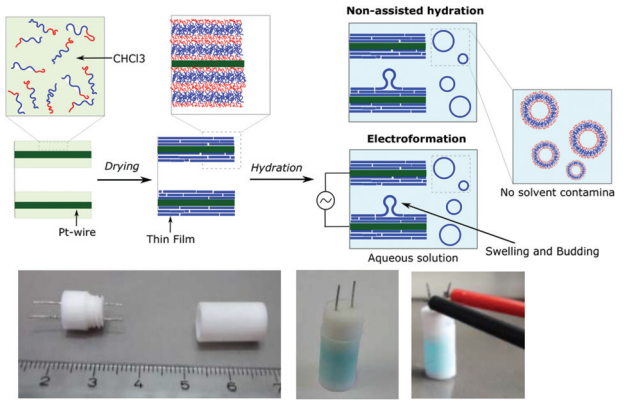


**Fig. 2** Electrochambers and electroformation methodology. (a) Scheme of non-assisted film hydration and electroformation methods. (b) Picture of the open homemade electro-chamber (left), the closed chamber after filling here with aqueous sucrose solution doped with $AF^{647}$ as used in the non-assisted film hydration method (middle) and then connected to the generator for electroformation (right).

Most surprisingly, control experiments showed that the same polymers ($PB_{73}$-*b*-$PEEP_{12}$ **A** and $PB_{73}$-*b*-$PEEP_{21}$ **B**) could also spontaneously self-assemble into GUVs in the absence of an alternating current within the same time period (1 h) on Pt-wires and on glass slides. All the other PB-*b*-PEEPs did not self-assemble into GUVs under these conditions. Non-assisted film hydration in such a fast timescale to form GUVs has never been reported before. Even in the case of lipidic GUVs, gentle hydration has only rarely been described as it requires long swelling times (typically several hours to days), is highly sensitive to any form of agitation, is unsuccessful for many amphiphiles and forms multilamellar deformed vesicles.[38,49,50] For polymersomes, reports even state that they have high energy requirements towards their self-assembly.[51] Control experiments for the formation of GUVs involving electroformation have not been explicitly described in previous studies.[35,40,41] Dimova *et al.* reported that the time required to form GUVs is much longer (3 h) at lower voltage (800 mV) and this resulted in smaller vesicles than those for 15 min at 9 V yielding GUVs of 40 μm radius on average.[38] The authors also showed that simple swelling, on Teflon surfaces, of PB-*b*-PEO and PEE-*b*-PEO took 3 days and resulted in smaller vesicles. Therefore, our fast non-assisted film hydration of PB-*b*-PEEPs into GUVs is unprecedented.

In order to compare the GUV formation between non-assisted film hydration (na-FH) and electroformation (EF), we quantified the yield (the number of GUVs formed) and their

**Table 1** Library of synthesized PB-*b*-PEEPs with a hydrophilic fraction $f$, $0.13 \leq f \leq 0.54$

| Entry | Polymer[a] | $f$[b] | $M_n$[a] | $Đ$[c] |
|---|---|---|---|---|
| 1 | $PB(1,4)_{73}$-*b*-$PEEP_4$ | 0.13 | 5000 | 1.07 |
| 2 | $PB(1,4)_{73}$-*b*-$PEEP_7$ | 0.21 | 5000 | 1.13 |
| 3 | $PB(1,4)_{73}$-*b*-$PEEP_{12}$ | 0.32 | 6000 | 1.14 |
| 4 | $PB(1,4)_{73}$-*b*-$PEEP_{21}$ | 0.45 | 7000 | 1.19 |
| 5 | $PB(1,4)_{73}$-*b*-$PEEP_{31}$ | 0.54 | 9000 | 1.17 |

[a] Degree of polymerization and $M_n$ were determined by NMR. [b] Hydrophilic fraction defined as $f$ = $M_n$(hydrophilic block)/$M_n$(block copolymer). [c] $Đ$, the molar mass dispersity, was determined by GPC.

mean diameters. In analogy to the well-established standard mammalian cell counting methods using a hemocytometer,[52] we manually counted the vesicles present in a number of random locations at the bottom of the well from microscopy images at a magnification of 20×. A magnification of 20× allows the counting to be done on an area of $6.4 \times 10^5$ μm$^2$ (divided into 16 squares of 200 μm length to ease counting – ESI† pS23) and was found it to be optimal for evaluating the vesicles formed. The number of vesicles at each location was then averaged out and back calculated to the vesicular yield obtained in the electro-chamber in GUVs per μL. Similarly, to the cell counting method, our yield estimation is prone to errors. For example, despite the density difference used between the inner phase (sucrose) and the outer phase (glucose), not all vesicles settled to the bottom where we counted them. We controlled that only a small proportion of vesicles could be found floating in the wells and no significant discrepancy was observed between settling times as long as a short 10 min latent period was given. Most importantly, for polymers that showed little to no vesicles, no vesicles were also observed floating and no changes in the results were reported at later times that could account for slower settling of the vesicles. Thus, it seems that the assumption that the majority of vesicle settle at the bottom rapidly does not have a significant impact on the estimated yield. Other parameters such as the number of vesicles transferred to the well, the location analyzed in the well, and counting errors, as well as experimental parameters such as film formation, the electro-chamber used and room conditions (temperature and humidity) could also affect the number of vesicles observed. The effect of these parameters can be minimized by systematically repeating the same protocol. In order to obtain a realistic yield estimation, we counted the cells at many different locations in the well (>5), replicated the experiments at least in triplicates and calculated the standard deviation between replicates. We also measured the diameter of each vesicle in order to determine the mean diameter of the vesicles per replicate. We then calculated the average of the mean diameters over the triplicate and their respective standard deviation. Finally, in analogy to dynamic light scattering (DLS) analysis of nanosized particles,[53,54] we calculated the polydispersity (PDI) as PDI = (standard deviation/mean diameter)$^2$ for each replicate and then calculated the average PDI. The average yield and their standard deviation, the mean diameter and their standard deviation and their respective average PDI are summarized in Table 2.

We observed that $PB_{73}$-*b*-$PEEP_{12}$ (entry 1) and $PB_{73}$-*b*-$PEEP_{21}$ (entry 2) clearly outperform the commonly used $PB_{46}$-*b*-$PEO_{23}$ ($f$ = 0.29) (entry 3),[55–58] $PDMS_{67}$-*b*-$PEO_{48}$ ($f$ = 0.30) (entry 4),[59,60] $PDMS_{60}$-*b*-$PMOXA_{21}$ ($f$ = 0.29) (entry 5),[61–63] and $PMOXA_{22}$-*b*-$PDMS_{119}$-*b*-$PMOXA_{22}$ ($f$ = 0.31) (entry 6)[36,64–67] in both EF and na-FH (ESI Table S1† for details of the replicated GUV yield). $PB_{73}$-*b*-$PEEP_{12}$ and $PB_{73}$-*b*-$PEEP_{21}$ gave similar high yields for both na-FH and EF (400 GUVs per μL and 175 GUVs per μL, respectively), typically giving a phase contrast image as seen in Fig. 3a. On the other hand, $PB_{46}$-*b*-$PEO_{23}$ (entry 3), $PDMS_{67}$-*b*-$PEO_{48}$ (entry 4) and $PMOXA_{22}$-*b*-$PDMS_{119}$-*b*-$PMOXA_{22}$ (entry 6) did not yield any GUVs by na-FH while $PDMS_{60}$-*b*-$PMOXA_{21}$ (entry 5) gave a low yield (4.77 ± 4.61 GUVs per μL). $PB_{46}$-*b*-$PEO_{23}$ (entry 3) and $PDMS_{60}$-*b*-$PMOXA_{21}$

**Table 2** Comparison of the yield of non-assisted film hydration (na-FH) and electroformation (EF) of various block copolymers

| Entry | Polymer | Yield (GUVs per μL)[a] | Mean Ø[b] (μm) | PDI[c] |
|---|---|---|---|---|
| 1 | $PB_{73}$-*b*-$PEEP_{12}$ | 355 ± 186 | 20 ± 2 | 0.78 |
| | | 161 ± 47 | 16 ± 4 | 0.80 |
| 2 | $PB_{73}$-*b*-$PEEP_{21}$ | 452 ± 144 | 14 ± 2 | 0.59 |
| | | 181 ± 70 | 16 ± 2 | 0.67 |
| 3 | $PB_{46}$-*b*-$PEO_{23}$ | 0.00 ± 0.00 | — | - |
| | | 3.54 ± 3.23 | 37 ± 11 | 0.35 |
| 4 | $PDMS_{67}$-*b*-$PEO_{48}$ | 0.00 ± 0.00 | — | — |
| | | 0.00 ± 0.00 | | |
| 5 | $PDMS_{60}$-*b*-$PMOXA_{21}$ | 4.77 ± 4.61 | 23 ± 4 | 0.20 |
| | | 4.00 ± 2.72 | 27 ± 17 | 0.33 |
| 6 | $PMOXA_{22}$-*b*-$PDMS_{119}$ -*b*-$PMOXA_{22}$ | 0.00 ± 0.00 | — | — |
| | | 0.00 ± 0.00 | | |

[a] Determined by phase contrast optical microscopy. [b] The mean diameter. [c] Polydispersity index defined as the average of the (standard deviation/mean)$^2$. For more details, the GUV yields for each replicate can be found in ESI Table S1 and their diameter and PDI in Tables S11–25, including frequency diagrams for their size distributions (Fig. S10–12).

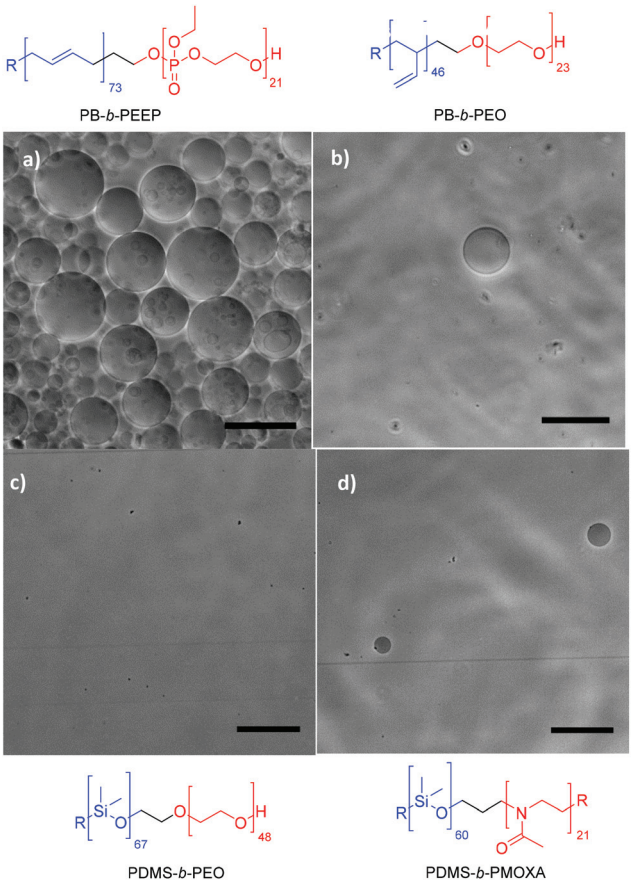


**Fig. 3** Typical phase contrast microscopy image of (a) $PB_{73}$-*b*-$PEEP_{12}$, (b) $PB_{46}$-*b*-$PEO_{23}$, (c) $PDMS_{67}$-*b*-$PEO_{48}$, and (d) $PDMS_{60}$-*b*-$PMOXA_{21}$ by film hydration. Scale bar: 100 μm.

(entry 5) gave a few GUVs using EF (<5 GUV per μL) contrary to $PDMS_{67}$-*b*-$PEO_{48}$ and $PMOXA_{22}$-*b*-$PDMS_{119}$-*b*-$PMOXA_{22}$ (Fig. 3b–d). Similar PB-*b*-PEOs with a variety of properties tested such as $0.2 \leq f \leq 0.4$ and $3000 \leq M_n \leq 17\,000$ also failed to produce GUVs by EF (ESI Table S1†) despite the frequent recurrence of PB-*b*-PEO in the formation of SUV and even GUV by various other methods.[37,42,55,58] In the same perspective, Mingotaud and coworkers also expressed difficulties in obtaining polymersomes with PB-*b*-PEO by EF on ITO plates and its narrow hydrophilic ratio range[37] as well as Greene *et al.* by EF on Pt wires.[42] Interestingly, despite the common assumption that EF improves the vesicular self-assembly,[12,68] we did not observe such an improvement for any of the block copolymers used and na-FH performed even slightly better for PB-*b*-PEEPs. We hypothesized that EF results in a smaller number of GUVs than na-FH as the electrical current might catalyze the degradation of GUVs perhaps by altering the polymer structure, in parallel with the previously studied degradation of polyunsaturated phospholipids.[69–71]

In terms of size, all samples had a large size distribution (PDI > 0.2); nonetheless, the replicates consistently gave the same mean diameters. The mean diameter was 20 ± 2 μm for $PB_{73}$-*b*-$PEEP_{12}$ **A** and 14 ± 2 μm for $PB_{73}$-*b*-$PEEP_{21}$ **B** during na-FH (the error representing the mean diameter uncertainty between replicates). Tuning the GUVs' size by EF to larger monodisperse vesicles was not observed, giving identical sizes and PDI to na-FH. In the case of $PB_{46}$-*b*-$PEO_{23}$, the mean diameter was 37 ± 11 μm, a significantly larger diameter than that for PB-*b*-PEEPs and $PDMS_{60}$-*b*-$PMOXA_{21}$. PB-*b*-PEEPs gave an apparent Gaussian distribution with a maximum at 5 μm (ESI Fig. S10–12†). Smaller vesicles than 1 μm were probably also formed but cannot be accounted for on the optical microscope. Experimentally, any object below 1 μm could not be definitely distinguished between vesicles or impurities by optical microscopy or SUVs be assessed by DLS due to the presence of GUVs, altering the scattering's statistical average.

In order to determine how long the GUVs self-assemble by na-FH, we conducted a kinetic study in triplicate with $PB_{73}$-*b*-$PEEP_{12}$ **A** (Fig. 4). We observed that the optimal vesicle number is achieved within 2 h, already achieving a large number of vesicles within 1 h (ESI Table S3†). The mean diameter of the vesicles decreased slightly over time from 23 ± 3 μm to 14 ± 1 μm, exemplifying that larger GUVs seem to be formed first (ESI Table S4†). Further na-FH experiments were thus carried out for 1 h in order to directly correlate EF and na-FH over the same timescale.

In the last decade, polymersomes have been increasingly used because of their inherent stability compared to liposomes.[24] Block copolymers are much less prone to chemical degradation than lipids and as they are larger molecules, entanglement in the bilayer can be greater, resulting in higher mechanical stability than that of liposomes.[14,47,67] We analyzed the size (ESI Tables S7 and S8† for more details) and yield evolution (Tables S5 and S6† for more details) of our PB-*b*-PEEP GUVs under no special storing conditions (kept in aqueous dispersion at room temperature). We observed for our

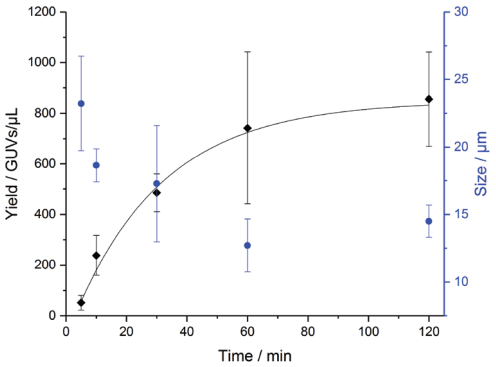


**Fig. 4** Formation of $PB_{73}$-*b*-$PEEP_{12}$ GUVs over time by non-assisted film hydration (na-FH) measuring the resulting yield in GUVs per μL (black) and the mean diameter of the vesicles in μm (blue). Details of the GUV yields and diameter for each replicate can be found in ESI Tables S3 and S4.†

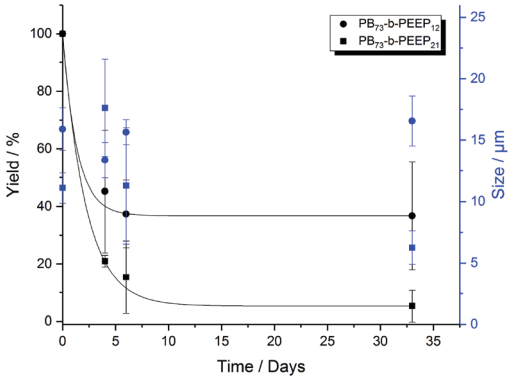


**Fig. 5** Yield (black) and size (blue) evolution over a period of 1 month of $PB_{73}$-*b*-$PEEP_{12}$ A and $PB_{73}$-*b*-$PEEP_{21}$ B. Details of the GUV yields and diameter for each replicate can be found in ESI Tables S5–8.†

PB-*b*-PEEPs that the vesicle yield slowly decreased (Fig. 5). After 1 month, 56 ± 10 GUVs per μL of vesicles were still present for $PB_{73}$-*b*-$PEEP_{12}$, thus effectively losing 63% in yield. In contrast, only 5% of $PB_{73}$-*b*-$PEEP_{21}$ remained. In terms of size, the mean diameter and size distribution of $PB_{73}$-*b*-$PEEP_{12}$ polymersomes over one month were similar to the freshly prepared GUVs, while the vast majority of $PB_{73}$-*b*-$PEEP_{21}$ were much smaller. For $PB_{73}$-*b*-$PEEP_{21}$, >80% of vesicle size was between 1 and 10 μm compared to 50% at the formation and with a mean diameter dropping to 6 ± 1 μm. Thus, it appears that $PB_{73}$-*b*-$PEEP_{12}$ GUVs are more stable than $PB_{73}$-*b*-$PEEP_{21}$ GUVs, influenced by a favored hydrophilic/hydrophobic block ratio.

Scaling up the film hydration protocol in a round bottom flask using 4 mg of polymer in 5 mL of aqueous sucrose solution (100 mM) was also successful. A similarly high number of GUVs for both PB-*b*-PEEP **A** and **B** was obtained in a round bottom flask, even whilst vigorously stirring, than in our small 350 μL-capacity reactors. These agitated film hydration protocols are most frequently used to obtain a large amount of poly-

dispersed multilamellar vesicles (MLV), usually <1 μm, which are then extruded through a polycarbonate membrane with small pores to obtain a homogeneous SUV population.[20,72,73] In the case of PB-*b*-PEEPs, many GUVs were obtained with diameters >25 μm, whilst PDMS-*b*-PEO and PMOXA-*b*-PDMS-*b*-PMOXA did not yield any GUVs, PB-*b*-PEO formed only a few GUVs (with smaller diameters of *ca.* 5 μm) and PDMS-*b*-PMOXA formed a small number of GUVs (20 μm).

### The polymers' physical properties

We wanted to determine why the PB-*b*-PEEP block copolymers formed a much higher number of GUVs than the classically used block copolymers. By analysis of the block themselves, we concluded that the hydrophobic block has a limited impact on the GUV yield as $PB_{74}$-*b*-$PEO_{45}$ with a similar degree of polymerization of PB, $M_n$ (6000 g mol$^{-1}$) and $f$ (0.33) to the successful $PB_{73}$-*b*-$PEEP_{12}$ yielded no vesicles. Thus, we believe that the hydrophilic block has the largest influence on vesicle formation.

During EF and na-FH, one of the crucial steps is polymeric film formation on Pt-electrodes; thus the block copolymers are in their neat state at ambient temperature before hydration. Depending on their inherent properties, polymers would stack and adhere to the surface differently, which would influence their subsequent self-assembly into vesicles. In order to assess these variations in the block copolymers, we ran differential scanning calorimetry (DSC). For vesicle formation, the block copolymers are first dissolved in $CHCl_3$ and then dried under reduced pressure once coated onto the Pt-wires. When treating our neat commercial PB-*b*-PEO in a similar way (dissolved in $CHCl_3$ at 4.0 mg mL$^{-1}$ and subsequently rapidly dried under reduced pressure), the DSC curve (ESI Fig. S7†) was similar to the second DSC heating curve of the neat polymer (Fig. S6†) and thus was analyzed as such for simplification.

Both $PB_{73}$-*b*-$PEEP_{12}$ **A** and $PB_{73}$-*b*-$PEEP_{21}$ **B** showed similar behavior: two $T_g$ at low values for both phase-separated blocks were determined (−97 °C and −59 °C for **A** (Fig. S4†) and −96 °C and −45 °C for **B** (Fig. S5†)) (Table 3). The lower $T_g$ at −90 °C corresponds to the PB block[20,74] while the $T_g$ around −50 °C corresponds to PEEP.[75] PB-*b*-PEEP are thus fully amorphous. By contrast, PB-*b*-PEO (Fig. S6†) and PDMS-*b*-PEO (Fig. S8†) both exhibited a melting temperature ($T_m$) of 33 °C and 51 °C, respectively (corresponding to PEO).[20] PB-*b*-PEO also has a single detectable $T_g$ at −60 °C. PDMS-*b*-PMOXA exhibited two $T_m$ at −41 °C and 60 °C (Fig. S9†). PB-*b*-PEO, PDMS-*b*-PEO, and PDMS-*b*-PMOXA are all thus semi-crystalline. At ambient temperature, at which the films are formed, all the commonly used block copolymers are below their $T_m$ and thus exhibit a crystalline-like packing.

The majority of EF studies rely on the operator's manual expertise in drop-cast film formation rather than automated methods like spin coating. Recently, Stein *et al.* suggested that non-uniform films (by manual drop-casting) might behave better than homogeneous films (for example, by spin-coating) as defects would allow a better water influx through the films, leading to facilitated GUV self-assembly.[71] The same assumption can be drawn to ordered partly crystalline block copolymers. The lack of defects present in the crystalline-like films in comparison with their disordered amorphous counterpart could alter the water infiltration within the films and consequently the formation of vesicles. The partly crystalline block copolymers would thus require a higher input of energy than the amorphous PB-*b*-PEEP to achieve similar levels of self-assembly into GUVs.[14,20,23,51] $PB_{46}$-*b*-$PEO_{23}$ could, therefore, form a few GUVs by EF but not by the milder na-FH methodology (Table 2, entry 3).

In the case of liposomes, self-assembly is always carried out at a temperature above the $T_m$ of the lipids.[68,76] We carried out the EF of PB-*b*-PEO at 50 °C, above its $T_m$, and obtained on average 1.7 ± 0.6 GUVs per μL, a yield similar to room temperature. Thus, contrary to lipids, modifying the temperature conditions does not change the behavior of PB-*b*-PEO in a manner that facilitates their self-assembly. PEO is known to have an inverse solubility–temperature relationship in aqueous solution with a lower critical solution temperature (LCST) typically >100 °C due to changes in its hydrogen bonding network with water.[77,78] It would therefore not be surprising that at elevated temperature, PB-*b*-PEO exhibits modified hydrophilicity behaviors inhibiting vesicular self-assembly.

We further analyzed the bulk morphology of PB-*b*-PEEP by transmission electron microscopy (TEM). Staining the double bonds of PB with $RuO_4$ was carried to observe the contrast between the hydrophilic and hydrophobic blocks. We observed that polymers **A** and **B** ($f$ = 0.32 and 0.45, respectively) exhibited extensive lamellar morphologies (Fig. 6 and ESI Fig. S13 and S14†). Interestingly, while the lamellar thickness was similar, the phase separation obtained with these polymers was inverted: $PB_{73}$-*b*-$PEEP_{12}$ **A** yielded PEEP thick lamellar structures (10.4 ± 1.3 nm for PEEP and 3.5 ± 0.4 nm for PB) whilst $PB_{73}$-*b*-$PEEP_{21}$ **B** yielded PB thick lamellar structures (11.0 ± 1.5 nm for PB and 4.4 ± 0.7 nm for PEEP). In contrast, $PB_{73}$-*b*-$PEEP_{31}$ ($f$ = 0.54) formed lamellar bulk structures (ESI Fig. S15†) but did not assemble into GUV. $PB_{73}$-*b*-$PEEP_4$ ($f$ = 0.13) and $PB_{73}$-*b*-$PEEP_7$ ($f$ = 0.21) did not form lamellar struc-

**Table 3** Comparison of the physical properties of block copolymers

| Block copolymer | $f$ | $\sigma^a$ (mN m$^{-1}$) | Thermal analysis$^b$ (°C) |
|---|---|---|---|
| $PB_{73}$-*b*-$PEEP_{12}$ | 0.32 | 8.96 ± 0.34 | $T_g$ = −97<br>$T_g$ = −59 |
| $PB_{73}$-*b*-$PEEP_{21}$ | 0.45 | 9.16 ± 0.15 | $T_g$ = −96<br>$T_g$ = −45 |
| $PB_{46}$-*b*-$PEO_{23}$ | 0.29 | 19.82 ± 0.49 | $T_g$ = −60<br>$T_m$ = 33 (30 J g$^{-1}$) |
| $PDMS_{67}$-*b*-$PEO_{48}$ | 0.30 | 19.80 ± 0.70 | $T_m$ = 51 (92 J g$^{-1}$) |
| $PDMS_{60}$-*b*-$PMOXA_{21}$ | 0.29 | —$^c$ | $T_m$ = −41 (8.0 J g$^{-1}$)<br>$T_m$ = 60 |

$^a$ Interfacial tension $\sigma$ measured by spinning drop tensiometry between $CHCl_3$ and $H_2O$ at a concentration of 1.0 mg mL$^{-1}$. $^b$ Measured by differential scanning calorimetry (DSC) between −100 °C and 100 °C. $^c$ The solution of PDMS-*b*-PMOXA in $CHCl_3$ could not be run as despite full dissolution the block copolymer crashes out during spinning in the tensiometer. Filtering with a PTFE 0.45 μm filter prior to $\sigma$ measurement did not limit that effect. The DSC curve for the thermal analysis can be found in ESI Fig. S4–9.

 

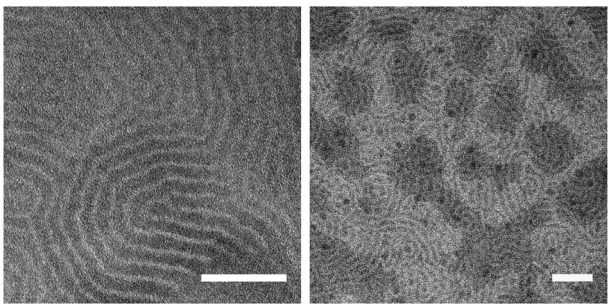

Fig. 6 Transmission electron microscopy (TEM) of $PB_{73}$-*b*-$PEEP_{21}$ films stained with $RuO_4$ exhibiting extensive lamellar networks. Scale bar: 100 nm.

tures as expected from block copolymer phase separation theory (ESI Fig. S16 and S17†).[46] $PB_{46}$-*b*-$PEO_{23}$ ($f$ = 0.29), which is well within the 0.25 < $f$ < 0.45 polymersome-forming range[11,48] but only yielded a small number of GUVs (Table 2, entry 3), did not form lamellar structures in the bulk (Fig. S18†). Thus, the presence of amorphous lamellar films in the bulk structure might ease the formation of GUVs.

Furthermore, we measured the interfacial tension $\sigma$ between $CHCl_3$ and $H_2O$ at a polymeric concentration of 1.0 mg $mL^{-1}$.The interfacial tension of $CHCl_3$ was determined to be 26.64 ± 0.67 mN $m^{-1}$. We observed that PB-*b*-PEEP lowers $\sigma$ to 8.96 ± 0.34 mN $m^{-1}$ for $PB_{73}$-*b*-$PEEP_{12}$ **A** and 9.16 ± 0.15 mN $m^{-1}$ for $PB_{73}$-*b*-$PEEP_{21}$ **B** while $PB_{46}$-*b*-$PEO_{23}$ and $PDMS_{67}$-*b*-$PEO_{48}$ gave 19.82 ± 0.49 mN $m^{-1}$ and 19.80 ± 0.70 mN $m^{-1}$, respectively. In comparison, the phospholipid POPC gave 3.90 ± 0.11 mN $m^{-1}$. POPC and, in general, other phospholipids are known to readily self-assemble into lipidic GUVs. Thus, a low interfacial tension might be an indication that amphiphiles (lipids and polymers) are more likely to form vesicles.

In addition, other properties of the block copolymers influence their self-assembly into vesicles such as hydrogen bonding. EEP is composed of four oxygen atoms, and thus it has eight available lone pairs that could form extensive hydrogen bonding networks. In contrast, PEO and PMOXA only have two and three available lone pairs, respectively, from oxygen or nitrogen atoms. This difference in hydrogen-bonding potential might also contribute to the success of PB-*b*-PEEPs. Moreover, PEEP and PMOXA allow delocalization of electrons onto O to form charged species that can also modify their adherence to Pt or glass surfaces and aid their self-assembly in aqueous solution.

### Encapsulation of hydrophilic and hydrophobic dyes

Ultimately, vesicles are interesting because of their compartmentalization, whether for chemical synthesis or biological mimicking. They are especially versatile compared to other carriers as they can encapsulate both hydrophilic and hydrophobic cargos with increasing complexity such as transmembrane proteins and even living cells.[32,79–81] These advanced encapsulations are almost exclusively carried out by microfluidics. Because of the nature of the methodology, encapsulation of hydrophilic moieties by film hydration techniques (EF, gel-assisted hydration) has been reported to be challenging even for liposomes.[14,20,76] Only sparse examples of passive encapsulation of hydrophilic cargos have been described for GUVs by film hydration. In the case of hydrophobic cargo, entrapment in the membrane has been well reported for polymersomes and liposomes.[14,40] Encapsulation of hydrophobic dyes is easier as the cargo is mixed with the amphiphilic agent prior to swelling and its entrapment in the membrane is entropically favored in aqueous media.

We first tested the encapsulation of the hydrophobic dye Nile Red (NR) (Table 4 and ESI Table S2† for more details). We define the encapsulation efficiency as the number of vesicles exhibiting fluorescence compared to the total number of vesicles observed in phase contrast (ESI† pS24). For both $PB_{73}$-*b*-PEEPs **A** and **B** (entries 1 and 2), using NR did not disrupt the vesicular yield and was even significantly improved for $PB_{73}$-*b*-$PEEP_{21}$ **B** to a high 1579 ± 279 GUVs per μL. Na-FH was again better at performing than EF, giving yields >580 GUVs per μL compared to 100–200 GUVs per μL for EF (Table 4, entries 1 and 2). Results for EF were similar to those in the absence of hydrophobic cargo. In the case of $PB_{46}$-*b*-$PEO_{23}$ (entry 3), similar low yields were obtained to those in the absence of dye: no GUVs were formed by na-FH and only a small number by EF (0.21 ± 0.36 GUVs per μL).

For all polymers, the encapsulation efficiency (ee) was optimal (all vesicles formed have encapsulated the hydrophobic dye in their membrane – Fig. 6 left). Thus, regardless of the block copolymer used, the encapsulation of NR has no effect or is improving the yield of vesicles obtained and the cargo can be efficiently encapsulated.

Encapsulation of the hydrophilic dye Alexa Fluor 647 ($AF^{647}$) was carried out by doping the aqueous sucrose medium with $AF^{647}$. Following hydration, the electro-chamber medium was then diluted into an $AF^{647}$-free glucose solution for observation. Thus any $AF^{647}$ in the extra-vesicular media is

Table 4 The yield of electroformation (EF) and non-assisted film hydration (na-FH) in the presence the hydrophobic dye Nile Red (NR) and the hydrophilic cargo Alexa Fluor 647 (AF)

| Entry | Polymer | Additive | Yield (GUVs per μL) | ee[a] (%) |
|---|---|---|---|---|
| 1 | $PB_{73}$-*b*-$PEEP_{12}$ | NR | 583 ± 101 | >99 |
| | | | 100 ± 36 | >99 |
| 2 | $PB_{73}$-*b*-$PEEP_{21}$ | | 1579 ± 279 | >99 |
| | | | 211 ± 106 | >99 |
| 3 | $PB_{46}$-*b*-$PEO_{23}$ | | 0.00 ± 0.00 | — |
| | | | 0.21 ± 0.36 | >99 |
| 4 | $PB_{73}$-*b*-$PEEP_{12}$ | $AF^{647}$ | 49 ± 11 | 46 ± 8 |
| | | | 117 ± 72 | 55 ± 15 |
| 5 | $PB_{73}$-*b*-$PEEP_{21}$ | | 74 ± 36 | 8 ± 3 |
| | | | 145 ± 128 | 23 ± 5 |

[a] Encapsulation efficiency. Defined as the number of vesicles expressing fluorescence over the total number of vesicles observed by phase contrast. Details of the GUV yields and ee for each replicate can be found in ESI Table S2.

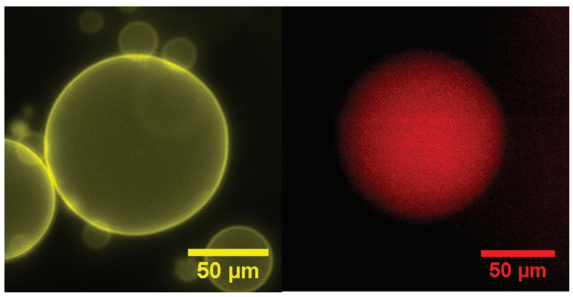


Fig. 7 Typical fluorescence microscopy image of PB-*b*-PEEPs of NR (left) and $AF^{647}$ (right) encapsulation.

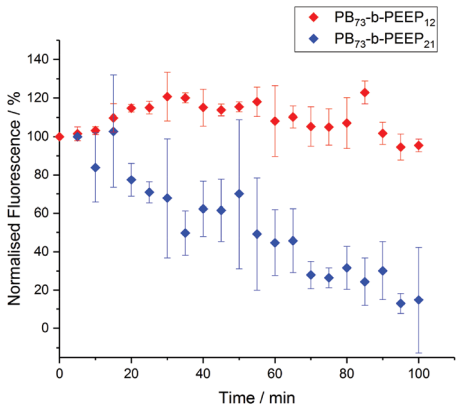


Fig. 8 $AF^{647}$ retention over time in GUVs based on the difference between the intravesicular emitted fluorescence and the background fluorescence. The fluorescence was normalized to 100% at $t$ = 0. Details of normalized fluorescence for each replicate can be found in ESI Tables S9 and S10.†

diluted by a factor of five and allows a contrast to be observed if $AF^{647}$ is encapsulated (Fig. 7 – right). When using $AF^{647}$ for passive encapsulation into PB-*b*-PEEP GUVs during na-FH, the yield significantly decreased: $PB_{73}$-*b*-$PEEP_{12}$ **A** produced only 49 ± 11 GUVs per µL and $PB_{73}$-*b*-$PEEP_{21}$ **B** 74 ± 36 GUVs per µL compared to typically 400 GUVs per µL (Table 4 and ESI Table S2† for more details). Thus hydrophilic cargo can have a strong negative influence on the self-assembly of the GUVs themselves. Small quantities of additives such as ions or salts have been shown to affect the self-assembly processes of SUVs to yield aggregates of various morphologies.[82,83] Thus it is not surprising that charged dyes like $AF^{647}$ would disturb GUV formation.

For EF, the yield of PB-*b*-PEEP GUVs in the presence of $AF^{647}$ was two times higher than for na-FH, giving similar values to the standard experiments in the absence of hydrophilic cargo (~100 GUVs per µL). In other EF studies, large frequencies (500 Hz) have been reported to compensate for ionic strength, such as charged lipids[36] or physiological buffers.[84,85] It is thus reasonable to conclude that the use of a moderate frequency (10 Hz) in our system is enough to compensate for the ionic strength of $AF^{647}$, impairing the spontaneous swelling of the polymeric films. This observation can also be correlated to the encapsulation of hydrophilic cargos by electroporation, a technique first tested on living cells.[51] We thus observed for the first time the beneficial effect of EF compared to na-FH when using PB-*b*-PEEPs.

The ee was higher than expected for $PB_{73}$-*b*-$PEEP_{12}$ **A** with a decent ~50% ee for both EF and na-FH, although generally, the fluorescence was weak. In the case of $PB_{73}$-*b*-$PEEP_{21}$ **B**, only low encapsulation (8 ± 3%) was obtained by na-FH. EF slightly improved the encapsulation to 23 ± 5%. Therefore, hydrophilic dyes are indeed harder to encapsulate than hydrophobic dyes; nonetheless, we were able to obtain a decent encapsulation efficiency when using $PB_{73}$-*b*-$PEEP_{12}$ **A**.

Polymersomes have been described to be less permeable than liposomes due to a much lower membrane fluidity.[24,86–88] This allows polymersomes to retain hydrophilic cargo and thus makes them promising candidates for protocells. In order to assess the permeability of the PB-*b*-PEEP vesicles, we analyzed the evolution over time of the intravesicular $AF^{647}$ fluorescence (Fig. 8, ESI Tables S9 and 10†). Vesicles of $PB_{73}$-*b*-$PEEP_{12}$ **A** appeared to be relatively hermetic with their fluorescence oscillating around 100% over 100 min, retaining $AF^{647}$ in the polymersome's lumen. $PB_{73}$-*b*-$PEEP_{21}$ **B** GUVs are more permeable, losing 85% fluorescence during the first 100 min. These results might also explain why the ee of $AF^{647}$ in GUVs of **B** was significantly lower compared to GUVs prepared from **A**, rendering **A** a promising candidate for generating protocells.

## Summary

We successfully synthesized a library of novel amphiphilic block copolymers (polybutadiene-*block*-poly(ethyl ethylene phosphate) (PB-*b*-PEEP)), with a polyphosphoester as the hydrophilic segment, resembling phospholipid-like structures for protocell assembly. PB-*b*-PEEPs with hydrophilic ratios of 0.32 and 0.45 successfully self-assembled into solvent- and additive-free GUVs with high yields by electroformation and non-assisted direct film hydration, *i.e.* in the absence of an alternating current or any other energy forces. In contrast to classically used block copolymers for polymersome formation, which are PB-*b*-PEO, PDMS-*b*-PEO, and PDMS-*b*-PMOXA block copolymers, we observed that polyphosphoester-based amphiphiles produced GUVs by spontaneous film hydration or electroformation very efficiently. Stability experiments proved that PB-*b*-PEEP GUVs could be stored at room temperature for several weeks. Furthermore, we proved that hydrophobic and hydrophilic cargos were encapsulated into the GUVs. Hydrophobic dyes were efficiently encapsulated by non-assisted film hydration. Hydrophilic dyes tested with $AF^{647}$ were more challenging to encapsulate into the GUVs. Nevertheless, 50% encapsulation efficiency could be achieved in $PB_{73}$-*b*-$PEEP_{12}$ GUVs and could be efficiently retained in the polymersomes for at least 2 h.

The straightforward synthesis of well-defined PB-*b*-PEEP block copolymers, their structural similarities to phospholipids, and the ease of producing loaded GUVs by simple film hydration make them promising new materials for the generation of protocells and microreactors.

## Conflicts of interest

There are no conflicts to declare.

## Acknowledgements

This work is part of the MaxSynBio consortium, which is jointly funded by the Federal Ministry of Education and Research of Germany and the Max Planck Society. We would like to thank Kathrin Kirchhoff and Dr Ingo Lieberwirth (MPIP) for TEM measurements. Open Access funding provided by the Max Planck Society.

## Notes and references

1 M. Li, X. Huang, T. Y. D. Tang and S. Mann, *Curr. Opin. Chem. Biol.*, 2014, **22**, 1–11.
2 M. C. M. van Oers, F. P. J. T. Rutjes and J. C. M. van Hest, *Curr. Opin. Biotechnol.*, 2014, **28**, 10–16.
3 A. I. Lamond, *Nature*, 2002, **417**, 383–383.
4 Y. Tu, F. Peng, A. Adawy, Y. Men, L. K. Abdelmohsen and D. A. Wilson, *Chem. Rev.*, 2016, **116**, 2023–2078.
5 B. C. Buddingh and J. C. M. van Hest, *Acc. Chem. Res.*, 2017, **50**, 769–777.
6 K. Gopfrich, I. Platzman and J. P. Spatz, *Trends Biotechnol.*, 2018, **36**, 938–951.
7 L. K. Müller and K. Landfester, *Biochem. Biophys. Res. Commun.*, 2015, **468**, 411–418.
8 V. Balasubramanian, B. Herranz-Blanco, P. V. Almeida, J. Hirvonen and H. A. Santos, *Prog. Polym. Sci.*, 2016, **60**, 51–85.
9 X. L. Hu, Y. G. Zhang, Z. G. Xie, X. B. Jing, A. Bellotti and Z. Gu, *Biomacromolecules*, 2017, **18**, 649–673.
10 H. L. Che and J. C. M. van Hest, *J. Mater. Chem. B*, 2016, **4**, 4632–4647.
11 D. E. Discher and F. Ahmed, *Annu. Rev. Biomed. Eng.*, 2006, **8**, 323–341.
12 A. Jesorka and O. Orwar, *Annu. Rev. Anal. Chem.*, 2008, **1**, 801–832.
13 J. F. Le Meins, C. Schatz, S. Lecommandoux and O. Sandre, *Mater. Today*, 2013, **16**, 397–402.
14 L. Messager, J. Gaitzsch, L. Chierico and G. Battaglia, *Curr. Opin. Pharmacol.*, 2014, **18**, 104–111.
15 V. Malinova, S. Belegrinou, D. D. Ouboter and W. P. Meier, *Adv. Polym. Sci.*, 2010, **224**, 113–165.
16 B. Clément, B. Grignard, L. Koole, C. Jérôme and P. Lecomte, *Macromolecules*, 2012, **45**, 4476–4486.
17 K. N. Bauer, H. T. Tee, M. M. Velencoso and F. R. Wurm, *Prog. Polym. Sci.*, 2017, **73**, 61–122.
18 F. Wang, Y.-C. Wang, L.-F. Yan and J. Wang, *Polymer*, 2009, **50**, 5048–5054.
19 T. Wolf, T. Rheinberger, J. Simon and F. R. Wurm, *J. Am. Chem. Soc.*, 2017, **139**, 11064–11072.
20 P. Walde, K. Cosentino, H. Engel and P. Stano, *ChemBioChem*, 2010, **11**, 848–865.
21 S. So, L. J. Yao and T. P. Lodge, *J. Phys. Chem. B*, 2015, **119**, 15054–15062.
22 R. S. M. Rikken, H. Engelkamp, R. J. M. Nolte, J. C. Maan, J. C. M. van Hest, D. A. Wilson and P. C. M. Christianen, *Nat. Commun.*, 2016, **7**, 12606.
23 P. V. Pawar, S. V. Gohil, J. P. Jain and N. Kumar, *Polym. Chem.*, 2013, **4**, 3160–3176.
24 E. Rideau, R. Dimova, P. Schwille, F. R. Wurm and K. Landfester, *Chem. Soc. Rev.*, 2018, DOI: 10.1039/c8cs00162f.
25 M. Chemin, P. M. Brun, S. Lecommandoux, O. Sandre and J. F. Le Meins, *Soft Matter*, 2012, **8**, 2867–2874.
26 T. P. T. Dao, F. Fernandes, M. Er-Rafik, R. Salva, M. Schmutz, A. Brulet, M. Prieto, O. Sandre and J. F. Le Meins, *ACS Macro Lett.*, 2015, **4**, 182–186.
27 C. Martino and A. J. deMello, *Interface Focus*, 2016, **6**, 20160011.
28 J. Petit, I. Polenz, J. C. Baret, S. Herminghaus and O. Baumchen, *Eur. Phys. J. E: Soft Matter Biol. Phys.*, 2016, **39**, 59.
29 J. Petit, L. Thomi, J. Schultze, M. Makowski, I. Negwer, K. Koynov, S. Herminghaus, F. R. Wurm, O. Baumchen and K. Landfester, *Soft Matter*, 2018, **14**, 894–900.
30 D. van Swaay and A. deMello, *Lab Chip*, 2013, **13**, 752–767.
31 T. P. T. Dao, M. Fauquignon, F. Fernandes, E. Ibarboure, A. Vax, M. Prieto and J. F. Le Meins, *Colloids Surf., A*, 2017, **533**, 347–353.
32 M. Weiss, J. P. Frohnmayer, L. T. Benk, B. Haller, J. W. Janiesch, T. Heitkamp, M. Borsch, R. B. Lira, R. Dimova, R. Lipowsky, E. Bodenschatz, J. C. Baret, T. Vidakovic-Koch, K. Sundmacher, I. Platzman and J. P. Spatz, *Nat. Mater.*, 2018, **17**(1), 89–96.
33 K. Tsumoto, H. Matsuo, M. Tomita and T. Yoshimura, *Colloids Surf., B*, 2009, **68**, 98–105.
34 T. J. Politano, V. E. Froude, B. Jing and Y. Zhu, *Colloids Surf., B*, 2010, **79**, 75–82.
35 B. M. Discher, Y. Y. Won, D. S. Ege, J. C. M. Lee, F. S. Bates, D. E. Discher and D. A. Hammer, *Science*, 1999, **284**, 1143–1146.
36 A. Weinberger, F. C. Tsai, G. H. Koenderink, T. F. Schmidt, R. Itri, W. Meier, T. Schmatko, A. Schroder and C. Marques, *Biophys. J.*, 2013, **105**, 154–164.
37 M. Dionzou, A. Morere, C. Roux, B. Lonetti, J. D. Marty, C. Mingotaud, P. Joseph, D. Goudouneche, B. Payre, M. Leonetti and A. F. Mingotaud, *Soft Matter*, 2016, **12**, 2166–2176.
38 R. Dimova, U. Seifert, B. Pouligny, S. Forster and H. G. Dobereiner, *Eur. Phys. J. E*, 2002, **7**, 241–250.
39 L. Theogarajan, S. Desai, M. Baldo and C. Scholz, *Polym. Int.*, 2008, **57**, 660–667.

40 A. M. Eissa, M. J. P. Smith, A. Kubilis, J. A. Mosely and N. R. Cameron, *J. Polym. Sci., Part A: Polym. Chem.*, 2013, **51**, 5184–5193.
41 A. Kubilis, A. Abdulkarim, A. M. Eissa and N. R. Cameron, *Sci. Rep.*, 2016, **6**, 32414.
42 A. C. Greene, I. M. Henderson, A. Gomez, W. F. Paxton, V. VanDelinder and G. D. Bachand, *PLoS One*, 2016, **11**, e0158729.
43 M. A. Hillmyer and F. S. Bates, *Macromolecules*, 1996, **29**, 6994–7002.
44 J. M. Chen, Z. J. Lu, G. Q. Pan, Y. X. Qi, J. J. Yi and H. J. Bai, *Chin. J. Polym. Sci.*, 2010, **28**, 715–720.
45 P. Patnaik, *A Comprehensive Guide to the Hazardous Properties of Chemical Substances*, Wiley, 2007.
46 Y. Y. Mai and A. Eisenberg, *Chem. Soc. Rev.*, 2012, **41**, 5969–5985.
47 X. Y. Zhang, P. Tanner, A. Graff, C. G. Palivan and W. Meier, *J. Polym. Sci., Part A: Polym. Chem.*, 2012, **50**, 2293–2318.
48 D. E. Discher and A. Eisenberg, *Science*, 2002, **297**, 967–973.
49 J. P. Reeves and R. M. Dowben, *J. Cell Physiol.*, 1969, **73**, 49–60.
50 N. Rodriguez, F. Pincet and S. Cribier, *Colloids Surf., B*, 2005, **42**, 125–130.
51 L. G. Wang, L. Chierico, D. Little, N. Patikarnmonthon, Z. Yang, M. Azzouz, J. Madsen, S. P. Armes and G. Battaglia, *Angew. Chem., Int. Ed.*, 2012, **51**, 11122–11125.
52 M. Absher, in *Tissue Culture*, Academic Press, 1973, pp. 395–397, DOI: 10.1016/B978-0-12-427150-0.50098-X.
53 Z. T. Qin, J. Joo, L. Gu and M. J. Sailor, *Part. Part. Syst. Charact.*, 2014, **31**, 252–256.
54 N. K. Kozlov, U. A. Natashina, K. P. Tamarov, M. B. Gongalsky, V. V. Solovyev, A. A. Kudryavtsev, V. Sivakov and L. A. Osminkina, *Mater. Res. Express*, 2017, **4**, 095026.
55 J. Gaspard, L. M. Casey, M. Rozin, D. J. Munoz-Pinto, J. A. Silas and M. S. Hahn, *Sensors*, 2016, **16**(3), 390.
56 H. L. Che, B. C. Buddingh' and J. C. M. van Hest, *Angew. Chem., Int. Ed.*, 2017, **56**, 12581–12585.
57 A. Peyret, E. Ibarboure, N. Pippa and S. Lecommandoux, *Langmuir*, 2017, **33**, 7079–7085.
58 A. Peyret, E. Ibarboure, J. F. Le Meins and S. Lecommandoux, *Adv. Sci.*, 2018, **5**, 1700453.
59 G. Kickelbick, J. Bauer, N. Huesing, M. Andersson and K. Holmberg, *Langmuir*, 2003, **19**, 10073–10076.
60 G. Kickelbick, J. Bauer, N. Husing, M. Andersson and A. Palmqvist, *Langmuir*, 2003, **19**, 3198–3201.
61 K. Jaskiewicz, M. Makowski, M. Kappl, K. Landfester and A. Kroeger, *Langmuir*, 2012, **28**, 12629–12636.
62 S. Winzen, M. Bernhardt, D. Schaeffel, A. Koch, M. Kappl, K. Koynov, K. Landfester and A. Kroeger, *Soft Matter*, 2013, **9**, 5883–5890.
63 K. Kiene, S. H. Schenk, F. Porta, A. Ernst, D. Witzigmann, P. Grossen and J. Huwyler, *Eur. J. Pharm. Biopharm.*, 2017, **119**, 322–332.
64 Y. R. Kim, S. Jung, H. Ryu, Y. E. Yoo, S. M. Kim and T. J. Jeon, *Sensors*, 2012, **12**, 9530–9550.
65 A. Najer, S. Thamboo, C. G. Palivan, H. P. Beck and W. Meier, *Chimia*, 2016, **70**, 288–291.
66 L. Klermund, S. T. Poschenrieder and K. Castiglione, *ACS Catal.*, 2017, **7**, 3900–3904.
67 S. T. Poschenrieder, S. K. Schiebel and K. Castiglione, *Eng. Life Sci.*, 2018, **18**, 101–113.
68 M. I. Angelova and D. S. Dimitrov, *Faraday Discuss.*, 1986, **81**, 303–311.
69 Y. Zhou, C. K. Berry, P. A. Storer and R. M. Raphael, *Biomaterials*, 2007, **28**, 1298–1306.
70 M. Breton, M. Amirkavei and L. M. Mir, *J. Membr. Biol.*, 2015, **248**, 827–835.
71 H. Stein, S. Spindler, N. Bonakdar, C. Wang and V. Sandoghdar, *Front. Physiol.*, 2017, **8**(63), DOI: 10.3389/fphys.2017.00063.
72 L. D. Mayer, M. J. Hope and P. R. Cullis, *Biochim. Biophys. Acta*, 1986, **858**, 161–168.
73 S. Vemuri and C. T. Rhodes, *Pharm. Acta Helv.*, 1995, **70**, 95–111.
74 G. Janowska and L. Slusarski, *J. Therm. Anal. Calorim.*, 2001, **65**, 205–212.
75 S. Zhang, J. Zou, F. Zhang, M. Elsabahy, S. E. Felder, J. Zhu, D. J. Pochan and K. L. Wooley, *J. Am. Chem. Soc.*, 2012, **134**, 18467–18474.
76 A. Akbarzadeh, R. Rezaei-Sadabady, S. Davaran, S. W. Joo, N. Zarghami, Y. Hanifehpour, M. Samiei, M. Kouhi and K. Nejati-Koshki, *Nanoscale Res. Lett.*, 2013, **8**, 102–111.
77 R. Kjellander and E. Florin, *J. Chem. Soc., Faraday Trans. 1*, 1981, **77**, 2053–2077.
78 F. Kafer, F. Liu, U. Stahlschmidt, V. Jerome, R. Freitag, M. Karg and S. Agarwal, *Langmuir*, 2015, **31**, 8940–8946.
79 R. Chandrawati and F. Caruso, *Langmuir*, 2012, **28**, 13798–13807.
80 F. Fernandez-Trillo, L. M. Grover, A. Stephenson-Brown, P. Harrison and P. M. Mendes, *Angew. Chem., Int. Ed.*, 2017, **56**, 3142–3160.
81 Y. Elani, T. Trantidou, D. Wylie, L. Dekker, K. Polizzi, R. V. Law and O. Ces, *Sci. Rep.*, 2018, **8**, 4564.
82 P. Bucher, A. Fischer, P. L. Luisi, T. Oberholzer and P. Walde, *Langmuir*, 1998, **14**, 2712–2721.
83 P. L. Soo and A. Eisenberg, *J. Polym. Sci., Part B: Polym. Phys.*, 2004, **42**, 923–938.
84 S. Aimon, J. Manzi, D. Schmidt, J. A. Poveda Larrosa, P. Bassereau and G. E. Toombes, *PLoS One*, 2011, **6**, e25529.
85 W. Zong, S. H. Ma, X. N. Zhang, X. J. Wang, Q. C. Li and X. J. Han, *J. Am. Chem. Soc.*, 2017, **139**, 9955–9960.
86 J. F. Le Meins, O. Sandre and S. Lecommandoux, *Eur. Phys. J. E: Soft Matter Biol. Phys.*, 2011, **34**, 14.
87 R. Dimova, in *Advances in Planar Lipid Bilayers and Liposomes*, ed. A. Iglič, Academic Press, 2012, vol. 16, pp. 1–50.
88 R. Dimova, *Adv. Colloid Interface Sci.*, 2014, **208**, 225–234.

 